Rare Met. (2022) 41(10):3574–3578
https://doi.org/10.1007/s12598-015-0599-x

RARE METALS

Chemical vapor deposition growth and transport properties of MoS_2–2H thin layers using molybdenum and sulfur as precursors

Zhi-Tian Shi, Hong-Bin Zhao, Xiao-Qiang Chen, Ge-Ming Wu, Feng Wei*, Hai-Ling Tu

Received: 8 August 2014 / Revised: 15 January 2015 / Accepted: 20 August 2015 / Published online: 18 September 2015
© The Nonferrous Metals Society of China and Springer-Verlag Berlin Heidelberg 2015

Abstract This paper introduces a feasible process to achieve the molybdenum disulfide atomic layers using chemical vapor deposition (CVD) method, with molybdenum thin film and solid sulfur as precursors. And some improvements were made to reduce the amount of metastable MoS_2–3R. The morphology of the acquired MoS_2 layers, existing as triangular flakes or large-area continuous films, can be controlled by adjusting the synthesis time and reacting temperature. The characterization results show that the monolayer MoS_2 flakes reveal a (002)-oriented growth on SiO_2/Si substrates, and its crystalline domain size is approximately 30 µm, and the thickness is 0.65 nm. Since the synthesis of MoS_2–3R is restrained, the electronic transport properties of MoS_2 with different layers were investigated, revealing that those properties equal with those of MoS_2 samples prepared by exfoliation methods.

Keywords Molybdenum disulfide; Chemical vapor deposition; Raman spectra; Atomic force microscope; Electronic transport properties

Z.-T. Shi, H.-B. Zhao, X.-Q. Chen, G.-M. Wu, F. Wei*
Advanced Electronic Materials Institute, General Research Institute for Nonferrous Metals, Beijing 100088, China
e-mail: jonthwei@hotmail.com

H.-L. Tu
National Engineering Research Center for Semiconductor Materials, General Research Institute for Nonferrous Metals, Beijing 100088, China

1 Introduction

Since graphene has many great physical [1–3] and electrical properties [4], it became the most widely studied two-dimensional material over the past decade [5, 6]. However, lacking of bandgap in pristine graphene greatly limits the application of graphene in electronic devices fabrication, for bandgap is the essential property for many applications, especially transistors. Transition metal chalcogenides (TMCs) exhibit a wide range of electronic, optical, and mechanical properties. Most importantly, they have bandgap, which makes them promising candidates for fabrication of field-effect transistors (FETs) and other electronic devices.

As a typical kind of TMCs, molybdenum disulfide in bulk form is semiconducting with an indirect bandgap of 1.2 eV [7], while monolayer MoS_2 has a direct bandgap of 1.8 eV [8] due to the dimensional confinement effects as the material becomes two-dimensional [9]. The bandgap energy change transforms the bandgap in monolayer MoS_2 into a direct bandgap, since the majority of electronic states near the K-point in the Brillouin zone are restricted within the layers, so that only slightly shift up in energy happens while the MoS_2 film thickness decreases. As a result, the monolayer material exhibits bright photoluminescence [10].

Non-equilibrium Green's function transport calculations show that MoS_2 atomic layer has a large on/off ratio of 1×10^{10} and is nearly immune to short-channel effects [11]. The mobility of monolayer MoS_2 can be tuned to above 200 $cm^2 \cdot V^{-1} \cdot s^{-1}$ using HfO_2 as dielectric layer in a top-gated MoS_2 FET, while the on/off ratio reaches up to 1×10^8 [12].

Owing to the merits of the MoS_2 mentioned above, exploring controllable ways of synthesizing large-area

MoS_2 is significantly important to the applications, and various approaches have been reported so far. In 1995, Feldman et al. [13] reported that MoS_2 nanofilm can be synthesized using chemical vapor deposition (CVD) method. Coleman et al. [14] achieved MoS_2 film by liquid exfoliation. Shi et al. [15] introduced epitaxy of MoS_2 layers in 2012. Liu et al. [16] presented thermal deposition method of MoS_2 films. Zhan et al. [17] synthesized large-area MoS_2 thin film using CVD method. However, the electrical property of artificially synthesized MoS_2 layers is relatively low compared to that of those MoS_2 flacks achieved through exfoliation. Hence, a more effective way is still pursuing. Considering that CVD method is suitable for large-area film synthesis, here it was presented a simple process for preparing shape-controllable MoS_2 layers using CVD method with molybdenum thin film and solid sulfur as precursors. The electronic transport properties of the MoS_2 reveal that those properties equal with those of MoS_2 samples prepared by other methods.

2 Experimental

2.1 Preparation of MoS_2 layers

Our new method was derived from a conventional process of MoS_2 synthesis. First, thin Mo film was deposited on SiO_2/Si substrate using magnetron sputtering (MS, SKY-60C15) from Mo metal target at room temperature with a power of 40 W. The thickness of SiO_2 on degenerately doped silicon substrate was 300 nm. Sputtering time was carefully adjusted to control Mo film thickness.

A quartz boat with samples (Mo films deposited on SiO_2/Si substrates) on was placed in the center of the quartz tube. A ceramic boat holding pure sulfur was placed in the upwind zone in quartz tube, where the temperature would remain a little above the melting point of sulfur (112.8 °C) after the center of the quartz tube was heated up to the growth temperature (750 °C). The quartz tube then would be loaded in a tube furnace with an offset toward the up-wind zone for 10 cm. The sulfur would not melt until quartz tube was pushed back to the precalculated position. The quartz tube was purged using high-purity N_2 at the flow rate of 100 $ml \cdot min^{-1}$ to form a protective atmosphere. After 30 min of N_2 purging, the system temperature gradually increased from room temperature to 450 °C, holding for 30 min to protect the furnace. The heat preservation at 450 °C also helps avoid any chance of Mo reacting with residual oxygen. Then, it was proceeded to heat the system from 450 °C to the optimum growth temperature of 750 °C. As the temperature of the sample increased again to 750 °C after the quartz tube was set back to the predetermined position, the temperature of whole system was then held for a certain period of time before cooled down to room temperature. The reaction time was determined by the requested kind of MoS_2 layers. Normally, the thin film appears in the form of triangular flakes holding the temperature for less than 10 min and continuous films holding the temperature for more than 30 min.

2.2 Transfer

The transfer method was also optimized to guarantee that the film can be transferred undamaged. The as-grown MoS_2 triangular flakes or continuous films on SiO_2/Si substrates can be transferred to arbitrary substrates by etching away the SiO_2 layer between MoS_2 nanolayers and silicon. Polymethylmethacrylate (PMMA) was spin-coated on the samples as support to avoid damage to the thin films. Samples were soaked into potassium hydroxide solution ($\sim$15 $mol \cdot L^{-1}$) in an alkali-resisting ceramic boat. The ceramic boat was heated to 60 °C to accelerate the reaction. When the MoS_2 layers were transferred, the sample was purified by dissolving the spin-on PMMA coating in acetone.

2.3 FETs fabrication

FETs were fabricated based on our presynthesized MoS_2 layers. A layer of photoresist was spin-coated on each sample. Location of triangular MoS_2 flakes formed on substrate was then confirmed by optical microscope (OM, Everbeing EB-6RF). After exposure and development, a pair of 150-nm gold electrodes was magnetron-sputtered on top of one particularly selected triangular MoS_2 flake.

2.4 Characterizations

The morphology was characterized by OM and atomic force microscope (AFM, Agilent Technologies 5100 ICP-OES). Raman and photoluminescence (PL, Horiba JYH-800) spectra were collected to confirm the layer number of MoS_2 samples. X-ray diffraction (XRD, RIGAKU smart-lab) patterns of the samples were used for identifying the orientation and quality of the crystal lattice. Electrical transport properties were characterized to reveal the intrinsic electrical properties of the MoS_2 films synthesized by this process.

3 Results and discussion

3.1 Morphology observation

Firstly, the as-synthesized triangular MoS_2 flakes (Fig. 1a) or continuous MoS_2 films (Fig. 1b) on SiO_2/Si substrates

were observed using OM. The size of an insulated triangular MoS_2 flake can reach up to more than 20 µm as shown in Fig. 1a.

AFM images of triangular MoS_2 flakes were taken to further study the morphology of monolayer MoS_2 (Fig. 2).

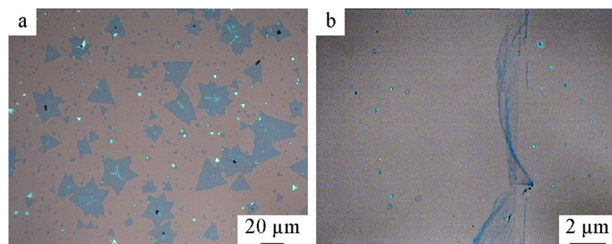

Fig. 1 OM images of MoS_2: **a** triangular flakes and **b** continuous film

The phase image in Fig. 2a shows that few wrinkles appear on MoS_2 flake. Besides, overlapping of MoS_2 monolayers are also found in Fig. 2a. The cross-section plot in Fig. 2b indicates that the thickness of monolayer MoS_2 is 0.65 nm, which matches with the crystal structure model. The morphology observation shows that monolayer MoS_2 can be achieved by this process.

To quantitatively determine the layer thicknesses, Raman spectra on as-prepared MoS_2 atomic layers were used (Fig. 3a). The system used for this work utilized a 532-nm laser. Low-power laser was used to protect the sample from decomposition. As illustrated in Fig. 3a, two typical Raman active modes could be found: E^1_{2g} (indicates planar vibration) and A_{1g} (associates with the vibration of sulfides in the out-of-plane direction) [18]. Blueshift for E^1_{2g} and redshift for A_{1g} are observed when MoS_2

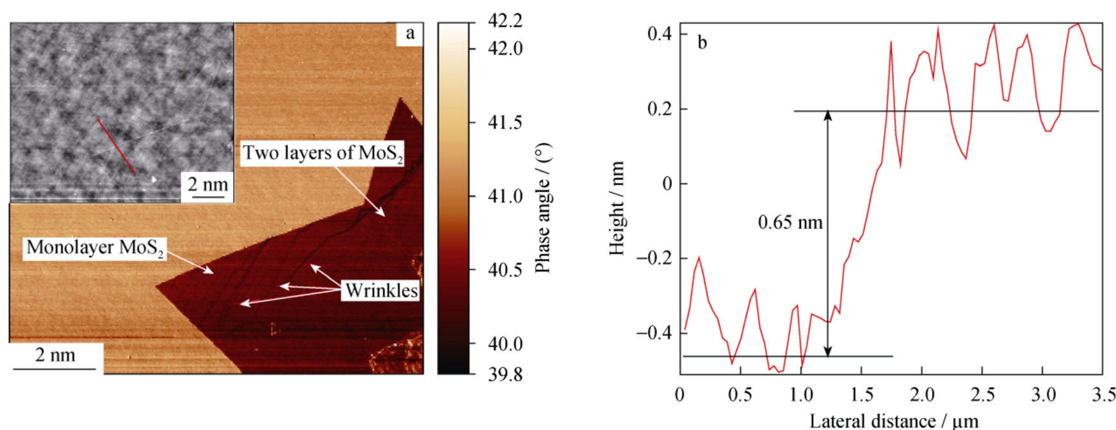

Fig. 2 AFM images of monolayer MoS_2: **a** phase image (inset: topography image) and **b** cross-sectional plot along red line in **a**

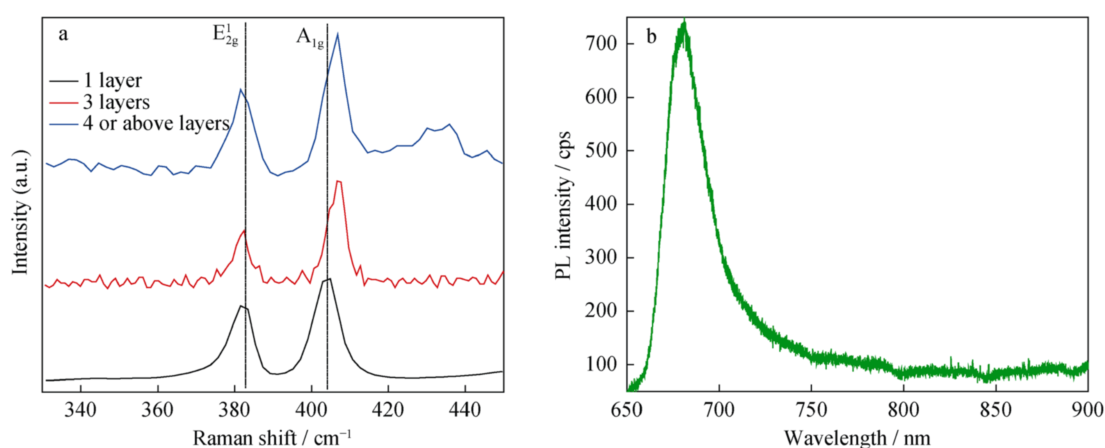

Fig. 3 Raman spectra of MoS_2 layers **a** and PL spectrum of monolayer MoS_2 **b**

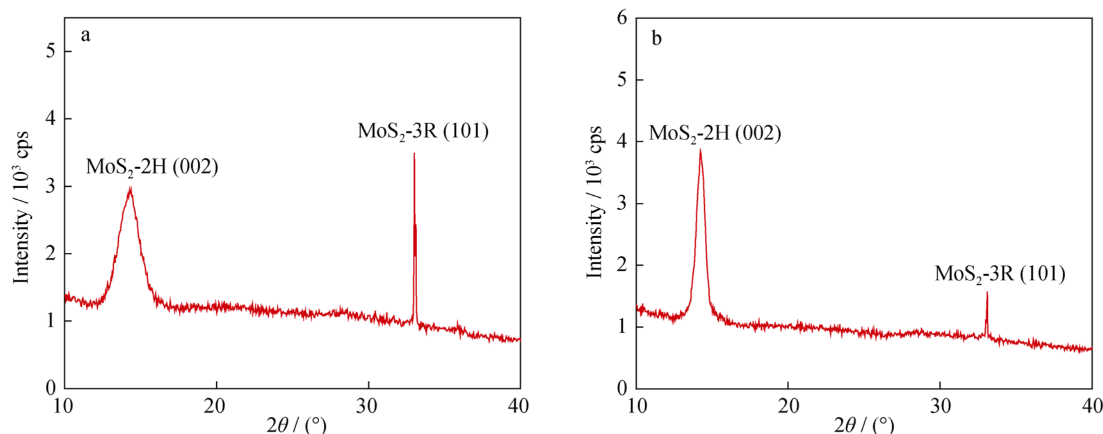

Fig. 4 XRD patterns of MoS_2 prepared by **a** ordinary CVD method and **b** this improved CVD method

layers become thinner. PL spectrum (Fig. 3b) contains one strong emission peak at about 690 nm. With Eq. (1), the bandgap (E) of the sample could be calculated.

$$E = h(c/\lambda) \quad (1)$$

where h stands for Planck constant, λ is the absorption wavelength of sample, and c is velocity of light. The absorption wavelength is known, so the bandgap of the MoS_2 sample is approximately 1.8 eV. The result further confirms that MoS_2 film is monolayer.

3.2 XRD results

The orientation of the MoS_2 crystals prepared by CVD method was determined by XRD. The XRD pattern in Fig. 4a was taken from MoS_2 sample synthesized by normal procedure, in which considerable amount of MoS_2–3R (101) are formed at a relatively low temperature before the synthesis of MoS_2–2H starts at 750 °C. It is notable that the MoS_2–3R molar quantity of the as-prepared MoS_2 layers by this improved process is effectively reduced, which can be proved by the XRD pattern in Fig. 4. In addition, the decrease in the full width at half maximum (FWHM) of MoS_2–2H peak also indicates that the crystalline quality of MoS_2 film is improved. The remaining MoS_2–3R can be easily turned into MoS_2–2H by annealing at a temperature of higher than 600 °C. MoS_2–2H layers tend to grow at (002) face on amorphous silicon dioxide.

3.3 Electronic transport properties

Electrical characterization of the devices was performed at room temperature using a Keithley 4200-SCS parameter analyzer. Schematic structure of as-fabricated FET is shown in Fig. 5a. The MoS_2 transistors with monolayer MoS_2 conductive channel are given a drain-source bias (V_{ds}) to the gold electrodes and back-gate voltage (V_{bg}) to the p + silicon substrate. The gating characteristics of the transistor are presented in Fig. 5b. These curves are typical of FET devices with n-type channel. The expression used for the mobility calculation is illustrated as Eq. (2):

$$\mu = \left[\mathrm{d}I_{ds}/\mathrm{d}V_{bg}\right] \times \left[L/(WC_iV_{ds})\right] \quad (2)$$

where $L = 20$ μm is the channel length, $W = 2$ μm is the channel width, I_{ds} is the current between the drain and the source, and $C_i = 1.17 \times 10^{-4}$ F·m^{-2} is the capacitance between the channel and the back gate per unit area ($C_i = \varepsilon_0\varepsilon_r/d$, $\varepsilon_r = 3.9$, $d = 300$ nm, where ε_0 is vacuum permittivity, ε_r is permittivity of the dielectric, and d is the thickness of the dielectric). The mobility of the first transistor is 0.03 × 0.01 cm^2·V^{-1}·s^{-1}.

FET with a three-layer MoS_2 channel was also fabricated and characterized by the same method. The characteristics are presented in Fig. 5c. Characteristic curves are also typical FET properties with n-type channel. The transistor with a thicker channel exhibits a higher mobility of (0.6 ± 0.1) cm^2·V^{-1}·s^{-1}.

Mobilities of both monolayer and three-layer MoS_2 samples are much lower than the theoretical value. The mobility of MoS_2 layers is suppressed by Coulomb scattering and phonon dispersion. The mobility can be improved by using high-κ (dielectric constant) materials as dielectric layer.

4 Conclusion

Triangular MoS_2 monolayer flakes and continuous MoS_2 atomic layers were synthesized by an improved CVD method. A combination of OM, XRD, AFM, and Raman spectra shows that those as-prepared MoS_2 layers present great quality, including inconsistent thicknesses and relatively large film areas. Preferred orientation of crystal growth on SiO_2/Si substrate is found. The content of

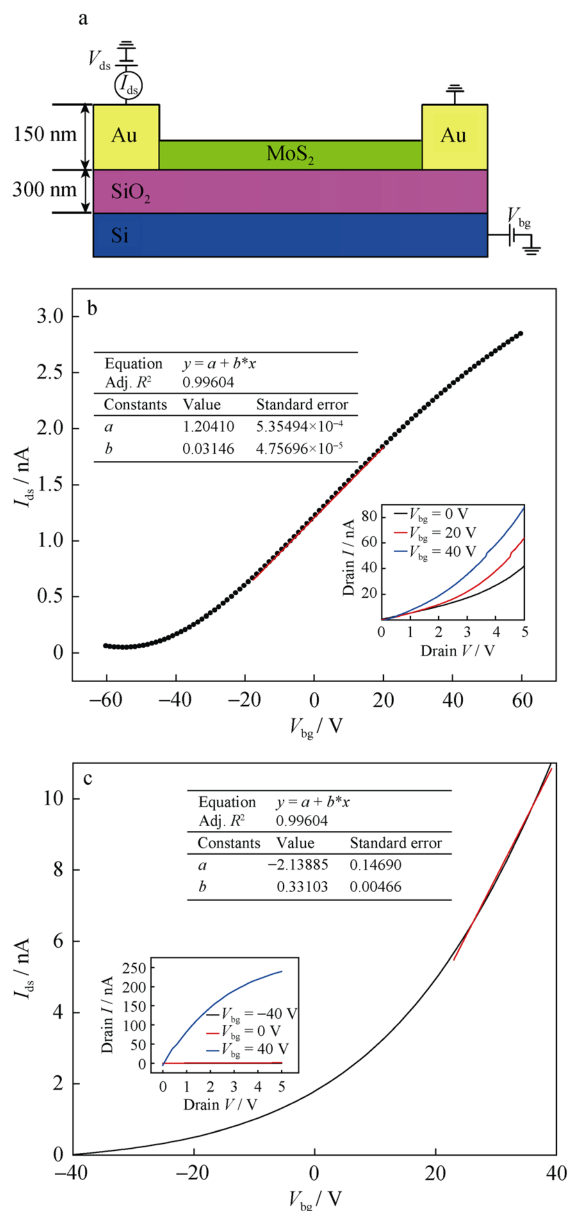

Fig. 5 Schematic structure of MoS_2-based FET **a**, gating characteristics of transistor **b**, and three-layer MoS_2 channel **c**

MoS_2–3R in the as-prepared MoS_2 can be restrained following the procedure presented in this paper. MoS_2-based FETs were fabricated to characterize the electrical transport properties. Mobility at room temperature ranges from 0.03 to 0.30 $cm^2 \cdot V^{-1} \cdot s^{-1}$, higher than those prepared by traditional methods. The result reveals that carrier mobility can be effectively improved by reducing MoS_2–3R content.

Acknowledgments This study was financially supported by the National Natural Science Foundation of China (Nos. 50835002 and 51105102).

References

[1] Novoselov KS, Geim AK, Morozov SV, Jiang D, Katsnelson MI, Grigorieva IV, Dubonos SV, Firsov AA. Two-dimensional gas of massless Dirac fermions in graphene. Nature. 2005;438(7065):197.

[2] Zhang YB, Tan YW, Stormer HL, Kim P. Experimental observation of the quantum Hall effect and Berry's phase in graphene. Nature. 2005;438(7065):201.

[3] Du X, Skachko I, Duerr F, Luican A, Andrei EY. Fractional quantum Hall effect and insulating phase of Dirac electrons in graphene. Nature. 2009;462(7270):192.

[4] Bolotina KI, Sikes KJ, Jianga Z, Klima M, Fudenberg G, Hone J, Kim P, Stormera HL. Ultrahigh electron mobility in suspended graphene. Solid State Commun. 2008;146(9):351.

[5] Novoselov KS, Geim AK, Morozov SV, Jiang D, Zhang Y, Dubonos SV, Grigorieva IV, Firsov AA. Electric field effect in atomically thin carbon films. Science. 2004;306(5696):666.

[6] Berger B, Song ZM, Li TB, Li CB, Ogbazghi AY, Feng R, Dai ZT, Marchenkov AN, Conrad EH, First PN, Heer WA. Ultrathin epitaxial graphite: 2D electron gas properties and a route toward graphene-based nanoelectronics. J Phys Chem B. 2004;108(52):19912.

[7] Kam KK, Parkinson BA. Detailed photocurrent spectroscopy of the semiconducting group VIB transition metal dichalcogenides. J Phys Chem. 1982;86(4):463.

[8] Mak KF, Lee C, Hone J, Heinz TF. Atomically thin MoS_2: a new direct-gap semiconductor. Phys Rev Lett. 2010;105(13):136805.

[9] Engel U, Eckstein R. Microforming-from basic research to its realization. J Mater Process Technol. 2002;125–126(9):35.

[10] Splendiani A, Sun L, Zhang Y, Li T, Kim J, Chim CY, Galli G, Wang F. Emerging photoluminescence in monolayer MoS_2. Nano Lett. 2010;10(4):1271.

[11] Yoon Y, Ganapathi K, Salahuddin S. How good can monolayer MoS_2 transistors be? Nano Lett. 2011;11(9):3768.

[12] Radisavljevic B, Radenovic A, Brivio J, Giacometti V, Kis A. Single-layer MoS_2 transistors. Nat Nanotechnol. 2011;6(3):147.

[13] Feldman Y, Wasserman E, Srolovitz DJ, Tenne R. High-rate, gas-phase growth of MoS_2 nested inorganic fullerenes and nanotubes. Science. 1995;267(5195):222.

[14] Coleman JN, Lotya M, O'Neill A, Bergin SD, King PJ, Khan U, Young K, De Gaucher AS, Smith RJ, Shvets IV, Arora SK, Stanton G, Kim HY, Lee K, Kim GT, Duesberg GS, Hallam T, Boland JJ, Wang JJ, Donegan JF, Grunlan JC, Moriarty G, Shmeliov A, Nicholls RJ, Perkins JM, Grieveson EM, Theuwissen K, McComb DW, Nellist PD, Nicolosi V. Two-dimensional nanosheets produced by liquid exfoliation of layered materials. Science. 2011;331(6017):568.

[15] Shi Y, Zhou W, Lu AY, Fang WJ, Lee YH, Hsu AL, Kim SM, Kim KK, Yang HY, Li LJ, Idrobo JC, Kong J. Van der Waals epitaxy of MoS_2 layers using graphene as growth templates. Nano Lett. 2012;12(6):2784.

[16] Liu KK, Zhang W, Lee YH, Lin YC, Chang MT, Su CY, Chang CS, Li H, Shi YM, Zhang H, Lai CS, Li LJ. Growth of large-area and highly crystalline MoS_2 thin layers on insulating substrates. Nano Lett. 2012;12(3):1538.

[17] Zhan Y, Liu Z, Najmaei S, Ajayan PM, Lou J. Large-area vapor-phase growth and characterization of MoS_2 atomic layers on a SiO_2 substrate. Small. 2012;8(7):966.

[18] Bertrand PA. Surface-phonon dispersion of MoS_2. Phys Rev B. 1991;44(11):5745.